RESEARCH ARTICLE

Surfactant-modified titania for cadmium removal and textile effluent treatment together being environmentally safe for seed germination and growth of *Vigna radiata*

Paromita Das[1,2] · Nupur Bahadur[2,3] · Vibha Dhawan[1,3]

Abstract

The present work describes synthesis, detailed characterization, and application of bare and surfactant-modified titania nanomaterials (NMs) for various wastewater treatment applications as individual cases like cadmium (Cd) removal, methylene blue (MB) dye degradation, and treatment of real textile and dyeing industry effluent. These NMs are used as adsorbents and photocatalysts in an indegenously developed end-to-end treatment process and a photocatalytic reactor for treatment of textile wastewater. The used NMs are suitably filtered and recovered for reuse; however, still this work focusses on the extent of potential risk and environmental safety of these engineered NMs towards seed germination and plant growth, in the event they escape wastewater treatment plants and reach out to natural water bodies and soil systems, accumulate over a period of time, and comes in contact with plant species. For synthesis, sol-gel method was utilized; cetyltrimethylammonium bromide (CTAB) and sodium dodecyl sulfate (SDS) were used as cationic and anionic surfactants, respectively, to act as particle growth templates and improve surface morphology. Detailed characterization involved XRD (X-ray diffraction), FTIR (Fourier-transform Infrared Spectroscopy), SEM (Scanning Electron Microscopy), TEM (Transmission Electron Microscopy), EDX (Energy Dispersive X-ray analysis), and BET (Brunauer-Emmett-Teller) surface area analysis. Improved morphology and surface properties, from irregular shape in Bare TiO_2 to spherical shape in surfactant-modified titania, led to enhanced Cd removal and MB dye degradation efficiency. Bare TiO_2 was used for complete treatment of textile wastewater, which took 5 h in achieving water quality, which is safe for discharge and reuse as per norms of Central Pollution Control Board (CPCB), Govt. of India. Phytotoxicity studies of these NMs at a wide concentration range (0–1000 mg L^{-1}) were undertaken towards *Vigna radiata*, and 500 mg L^{-1} concentration was found to be optimally safe for seed germination and plant growth.

Responsible editor: Gangrong Shi

✉ Nupur Bahadur
  nupur.bahadur@teri.res.in

1 Department of Biotechnology, TERI School of Advanced Studies, Plot No. 10 Institutional Area, Vasant Kunj, New Delhi 110070, India

2 TERI-Deakin Nano Biotechnology Centre, TERI Gram, The Energy and Resources Institute, Gual Pahari, Gurgaon Faridabad Road, Gurgaon, Haryana 122 001, India

3 The Energy and Resources Institute, Darbari Seth Block, India Habitat Center, Lodhi Road, New Delhi 110003, India

Introduction

Titanium dioxide has numerous applications in various fields of Science and Technology, and it is the method of synthesis which affects its properties and applications and ultimately the performance. Among several methods of synthesis, sol-gel is most preferred, due to its simplicity and ease; however, it leads to irregular shape and agglomeration of particles (Ganguli 1999). To prevent these, many approaches have been devised, among which modification with surfactants has shown promising results in terms of improved morphology and controlled particle size (Imae et al. 1991; Cassiers et al. 2004; Chai et al.

⚫ Springer

2007; Galkina et al. 2011; Tah et al. 2011; Bricha et al. 2012; Rashad and Shalan 2013; George et al. 2016; Wei et al. 2018; Wu et al. 2018). The surfactant-assisted systems regulates nucleation and growth of inorganic nanostructures which leads to increase in thermal stability, surface area, and aids in generation of active photocatalytic reaction sites, which acts as particle growth templates leading to mesoporous and higher surface area materials (Choi et al. 2010).

These modified titania nanomaterials have been used as adsorbents for heavy metal removal (Georgaka and Spanos 2010; Chawla et al. 2017; Dixit et al. 2017) and in particular for cadmium removal (Skubal et al. 2002; Zha et al. 2014; George et al. 2016). Sources of cadmium in the environment include natural weathering processes, by expulsion from industrial or sewage treatment plants and by leaching from landfills and atmospheric depositions. Cadmium can also be released into drinking water supplies from pipes in the water supply systems. Removal of Cadmium is particularly important because even at low concentration of exposure, it shows adverse chronic and acute effects on human body and ecological system (Jaishankar et al. 2014).

Zha et al. 2014 reported solvothermally prepared TiO_2 dandelions with 0.40 g g^{-1} Cd(II) monolayer adsorption capacity, where the hydroxyl groups on the surface of dandelions were responsible for Cd(II) adsorption (Zha et al. 2014). Skubal et al. 2002 reported the use of colloidal anatase TiO_2 (particle size 4.5 nm) to remove aqueous Cd(II) from simulated wastewaters. The titania surface was modified with bidental chelating agent thiolactic acid (TLA) as surfactants. Results indicated 20% Cd removal in the absence of light radiation following Freundlich adsorption isotherm, while 90% Cd removal by both adsorption and photocatalytic reduction processes onto the TLA-modified TiO_2 (Skubal et al. 2002).

Authors in their preliminary work on removal of various heavy metals like arsenic (As), chromium (Cr), lead (Pb), and cadmium (Cd) using bare and surfactant-modified titania reported cadmium (Cd) adsorption to be highest (George et al. 2016). The present work, therefore, aims to make complete understanding of the nature, behavior, and extent of Cadmium adsorption and removal efficiency on Bare, CTAB, and SDS-modified TiO_2.

Textile industry in India has been classified among the most polluting industry; effluents from this industry contains high amounts of color causing complex compounds, suspended solids, various oils, grease, surfactants, etc., whose treatment is a big challenge. Therefore there is need for innovative technologies like advanced oxidation (heterogeneous photocatalysis), where nanomaterials have been used as adsorbents and photocatalysts for dye degradation. There are several reports of photocatalysis on methylene blue (MB) dye degradation (Hattab et al. 2017; Dagher et al. 2018; Honarmand et al. 2019) and real textile industry effluent treatment (McKay et al. 1980; Nayana and Pushpa 2016; Sharma

and Kaur 2018). In this paper, we report bare and surfactant-modified titania for decolorization of MB dye and complete treatment of real textile effluent.

Another important aspect on which this study focusses is the risk assessment and ecosafety of titania towards seed germination and plant growth, in the event such engineered nanomaterials escape wastewater treatment plants (WWTPs) and reach out to natural water bodies and soil systems, accumulate over a period of time, and comes in contact with plants. Such a study holds vital importance, with regard to a report by Kiser et al. 2009 where nano and larger sized titania particles were found in soil around WWTPs. According to the report, at one of the WWTPs in Puerto Rico, it has been reported that raw sewage water contained 100 to nearly 3000 μg L^{-1} of titanium. The study also reported that titania particles larger than 0.7 μm accounted for the majority of the titania in raw sewage, and this fraction was well removed by WWTP processes. Titania concentrations in effluents from this and several other WWTPs ranged from 5 to 15 μg L^{-1} and were nearly all present in 0.7 μm size fraction (Kiser et al. 2009).

Hence along with concentration, the nature and particle size of exposed titania NPs towards phytotoxicity (seed germination and plant growth) is also essential to monitor and optimize. From earlier reports, it could be inferred that effects of TiO_2 exposure has been both positive (Kurepa et al. 2010; Dehkourdi and Mosavi 2013; Raliya et al. 2015; Singh et al. 2016; Jiang et al. 2017; Kořenková et al. 2017; Faraji and Sepehri 2018) and negative (Castiglione et al. 2014; Fellmann and Eichert 2017; Liu et al. 2017) towards seed germination and plant growth. TiO_2-based nanocomposites were reported to be accumulated and translocated to the shoots of *Arabidopsis thaliana* (thale cress) (Liu et al. 2017). Exposure of titania at both lower and higher concentrations have been reported to have opposite effects, e.g., low concentrations of n-TiO_2 in *Lactuca sativa* L. (lettuce) increased the root elongation whereas reduction in root growth at high concentration of 5000 mg L^{-1} of TiO_2 (Delaide et al. 2016). Another study on *Brassica campestris* (mustard) and *Phaseolus vulgaris* (common bean) shows no signs of toxicity even when they were exposed and treated with high concentration up to 5000 mg L^{-1} of TiO_2 (Larue et al. 2011); these studies indicate that nano-TiO_2 toxicity might vary in different plant species in different ways.

In this work, the synthesized bare and surfactant titania nanomaterials have been tested for seed germination and plant growth of mung bean (*Vigna radiata*) at different concentrations like 0, 50, 100, 250, 500, and 1000 mg L^{-1}, considering changes in various physiological parameters like shoot length, root length, vigor index, no. of leaves, color of leaves, etc. Thus this study holds vital importance in determining the effect of bare and surfactant-modified titania NMs towards various wastewater treatment applications and its potential risk

and environment safety aspect concerning seed germination and plant growth in *Vigna radiata*.

Experimental

Materials and methods

For synthesis of TiO_2 nanoparticles analytical grade chemicals like titanium tetraisopropoxide (TTIP) $\{Ti[OCH(CH_3)_2]_4\}$, ethanol (C_2H_5OH), hydrochloric acid (HCl), and surfactants like cetyltrimethylammonium bromide (CTAB) – $[C_{19}H_{42}BrN]$, and Sodium dodecyl sulfate (SDS) – $[CH_3(CH_2)_{11}SO_4Na]$ were all procured from Merck. For monitoring the ecosafety of these modified nanomaterials, the selected seeds of *Vigna radiata* (mung bean) were procured from Indian Agricultural Research Institute (IARI), New Delhi, India, which was further grown in water agar, and seeds were sterilized with 90% ethanol and 0.1% mercuric chloride procured from HiMedia.

Methodology for synthesis of bare and surfactant-modified titania

In the present work, Bare TiO_2, CTAB-modified TiO_2, and SDS-modified TiO_2 materials will be indicated throughout this manuscript as Bare TiO_2, CTAB-TiO_2, and SDS-TiO_2, respectively; these materials were synthesized following our earlier reported method (George et al. 2016), where 80 ml of ethanol (99% pure AR grade) was added to 12.5 ml of titanium tetraisopropoxide (TTIP) (284.22 g mL^{-1}, 97% pure AR grade) under continuous stirring, and the resultant solution was made up to 100 ml with 7.5 ml of deionized water. The solution was prepared under vigorous stirring for 2 h at room temperature, until a resulting clear solution was obtained, which was dried by heating at 100 °C for 30 min in the laboratory oven, and later the powders so obtained were annealed in muffle furnace at 550 °C at a heating rate of 8 °C min^{-1} to obtain desired TiO_2 powdered material. For modification of TiO_2, aqueous solutions of CTAB and SDS were added to the ethanolic solution of TTIP such that the effective concentration of each surfactant be 0.5 mM.

Figure 1 depicts synthesis approach of surfactant-modified TiO_2, where surfactant self-assembly is employed as particle growth templates. Upon a suitable concentration, surfactant molecules get self-organized and form reverse micelles with surfactant head group inside and tail group outside; when titanium isopropoxide precursor is hydrolyzed and condensed, it forms TiO_2 inorganic network in the water phase, inside the self-assembled surfactant, forming TiO_2 inorganic core/ surfactant organic shell structure. Upon annealing, organic templates are removed, and well-defined TiO_2 nanoparticles are formed.

Characterization of nanomaterial

The crystallographic analysis and detailed interpretation was done with Bruker D-8 advanced X-ray diffractometer using Cu-K$_\alpha$ wavelength ($\lambda = 1.54059$ Å) with scanning at 2θ between 20° to 70°. Fourier-transform infrared (FTIR) spectra of the nanomaterials were taken after making pallets in KBr and recorded on Nicolet iS50 FTIR spectrometer from Thermo Fisher Scientific. The surface topographical features and surface morphology of the synthesized nano-powders were studied using scanning electron microscope (SEM) (Carl Zeiss, Oberkochen, Germany). The particle size and crystallinity was examined using transmission electron microscope (TEM) (TECNAI G^2 T20 TWIN, FEI, Netherlands). The nitrogen adsorption-desorption isotherms were obtained on a Quantachrome Autosorb Automated Gas sorption system. All the samples were degassed at 150 °C prior to Brunauer-Emmett-Teller (BET) measurements. The BET-specific surface area was determined by a multipoint BET method with the adsorption data and the relative pressure P/P$_0$ range of 0.05–0.25. The desorption isotherm was used to identify the pore size using the Barrett-Joyner-Halenda (BJH) method with the nitrogen adsorption volume at P/P$_0 = 0.995$ for the determination of pore volume and average pore size. The
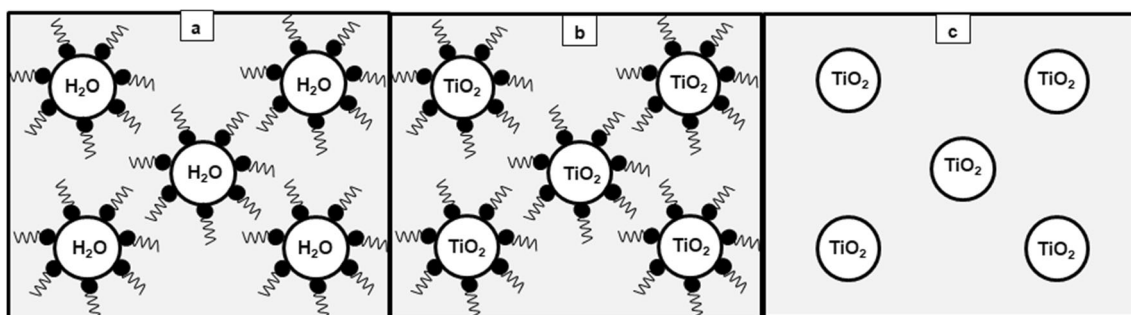

Fig. 1 Synthesis approach of surfactant modified TiO_2: (**a**) surfactant self-assembly as a particle growth template, (**b**) hydrolysis, and condensation of titanium isopropoxide precursor to form TiO_2 inorganic core/ surfactant organic shell structure (**c**) are formed after removal of the organic templates (Choi et al. 2010)

quantitative analysis of heavy metal ions was carried at mg L^{-1} level with atomic absorption spectrophotometer (iCE 3500, Thermo Fisher Scientific, USA) using reference standards (SCP Science, USA) after appropriate dilutions.

Adsorption of cadmium

In an earlier reported study by the group (George et al. 2016), four heavy metals were screened, i.e., As, Pb, Cd, and Cr towards adsorptive removal using Bare TiO_2. The % removal of As, Pb, Cd, and Cr was 40, 62, 75, and 10, respectively. Since Cd removal was highest, therefore it was chosen for detailed study. Also the effect of pH was studied for bare, CTAB, and SDS-modified TiO_2. It was concluded from this study that the optimum pH for Cd adsorption was 9.67, and it remained same for all three cases, which clearly established that the presence and nature of surfactant, i.e., cationic and anionic does not affect the adsorption behavior with the pH owing to all three materials primarily being pure titania.

The present work focuses on studying the extent and nature of adsorption of Cd on three materials in the concentration range of 1 to 12 mg dm^{-3} (mg L^{-1}) under the previously optimized conditions of pH 9.67, TiO_2 dosing of 0.1 g L^{-1} at 25 °C. Adsorption studies were carried out as described earlier and quantitatively analyzed as percentage removal efficiency by atomic absorption spectrophotometer (AAS-HG Vario-6-Analytik Jena, Germany). The study for removal of cadmium was carried out using reference standards (SCP Science, USA) after appropriate dilutions.

Photodegradation of methylene blue

For photocatalytic experiment, methylene blue (MB) was used as model pollutant dye. A 50 ml, 1×10^{-5} M aqueous solution of MB was taken, to which 0.1 g of powdered catalyst was mixed for 15 min in a beaker to obtain suspension, which was further left for 30 min to reach an adsorption/desorption equilibrium for MB in dark and later exposed in sunlight for an efficient photocatalytic action. The light exposure in all cases was 30 min from the time after adsorption. After 30 min, the samples were withdrawn and centrifuged (REMI Model R23) at the speed of 8000 rpm for 30 min to separate the catalyst. Then UV spectra of the centrifuged samples were recorded at 664 nm, which is the characteristic absorption peak of MB dye. Since the degradation pathways for the selected dye is well known, we have only monitored the decolorization process (Kumar et al. 2014).

Real textile effluent treatment

Raw textile and dyeing industry effluent was procured from an equalization tank of a cotton and polyester dyeing unit based in an Industrial area of Sonipat district of Haryana, India. The sample was treated immediately after receipt as per recently reported protocol (Bahadur and Bhargava 2019) which involved end-to-end treatment in three stages; first stage comprises of coagulation and flocculation using in-house-developed proprietary materials, followed by photocatalytic degradation of pollutant dyes in the effluent using Bare TiO_2 as the material. Used nanomaterial was recovered for further reuse, and clean-treated water was separated after suitable filtration. During the final stage of treatment, the treated water was passed through reverse osmosis (RO, membrane material and type – polyamide material and spirally bound type thin-film composite; Make – CSM, Korea and Model of RE4012-800) in order to emulate the current treatment already being practiced at commercial scale installations in India. Samples were sent to an accredited laboratory for wastewater characterization as per Standard Methods of Water and Wastewater Examination published by American Public Health Association, 23rd Edition, 2017.

Methodology for phytotoxicity test

Preparation of water agar medium

Water agar media was used for plant growth because it could support growth of the seeds at initial stages without any requirement of extra nutrients. About 20 g of agar was suspended in 1000 ml of distilled water. pH of the medium was adjusted to 5.8 by using dilute HCl and NaOH. It was heated in an oven up to 100 °C for 6–8 min until agar completely dissolved in water. Further it was sterilized by autoclaving for 15 min at 15 lbs pressure and 121 °C temperature. The medium was allowed to cool down to 50 °C for appropriate use. About 20 ml of the media was poured equally into each of the culture tubes (Barrett-Lennard and Dracup 1988).

Sterilization and soaking of seeds

The seeds of *Vigna radiata* were first washed with 90% ethanol for 10 min to ensure effective seed sterilization. They were then washed thoroughly 5–6 times with autoclaved double distilled water. Surface sterilization of seeds was carried out using 0.1% mercuric chloride for 30 s, and they were finally washed with autoclaved double distilled water 3–4 times in a laminar air flow chamber (Oyebanji et al. 2009).

Bare TiO_2 and SDS-TiO_2 nanomaterials were used for phytotoxicity studies; only SDS-TiO_2 was chosen among surfactant-modified materials because it showed highest adsorption capacity and removal efficiency of Cd as compared to CTAB-TiO_2. A wide concentration range of both types of the nanomaterials, Bare TiO_2, and as well as SDS-TiO_2 were chosen for phytotoxicity studies at the concentrations 50 mg L^{-1}, 100 mg L^{-1}, 250 mg L^{-1}, 500 mg L^{-1}, and 1000 mg L^{-1}.

Along with these, one sample in each case was controlled where there was no exposure of the either nanomaterial. The sterilized seeds of *Vigna radiata* were soaked for a period of 5 h in aqueous solutions of each of these NMs having specified concentrations in the solution. This soaking of seeds in the NMs solution lead to good absorption of NMs by the seed, which ultimately broke down the dormancy of the seed in order for seed to grow which was confirmed by the seed germination rate test following procedure by Jayarambabu et al. 2014 (N. Jayarambabu et al. 2014). The entire soaking process was carried out in beakers, which were covered by aluminum foil with holes made for providing ambient atmosphere. Mechanical shaking at the speed of 150 rpm was provided to all beakers during the entire soaking period so that a uniform shaking and stirring is achieved and also nanoparticles do not get settle down. After soaking, seeds were taken out and kept on autoclaved tissue paper to remove excess of solution around them.

Seed germination test

This test was conducted on *Vigna radiata* seeds. The seed germination rate (RSG), relative root growth (RRG), and germination index (GI) were calculated using the following formulas:

$$\text{Relative seed germination Rate} = (S_C/S_S) \times 100 \qquad (1)$$

$$\text{Relative root growth} = (R_S/R_C) \times 100 \qquad (2)$$

$$\text{Germination index} = (RSG/RRG) \times 100 \qquad (3)$$

where S_S is the number of seed germinated in sample, S_C is the number seed germinated in control, R_S is the average root length in sample, and R_C is the average root length in control.

In vitro studies of the NM-treated seeds

About 20 mL of culture media was taken in six culture tubes; one culture tube contained two seeds having no nanomaterial treatment, which is referred as control. To each of the remaining five tubes, two seeds each of the specified concentrations (50 mg L^{-1}, 100 mg L^{-1}, 250 mg L^{-1}, 500 mg L^{-1}, and 1000 mg L^{-1}) of Bare TiO_2 were inoculated. This exercise was performed in duplicates which means in each case, total four seeds were under study, i.e., $n = 4$. Hence in all, there were total 12 tubes having 24 seeds under study for Bare TiO_2. Similarly, the above procedure was performed with SDS-TiO_2 NM-treated seeds in duplicate. Hence in this case too, there were 12 tubes, having 24 seeds under study.

Care was taken to avoid any kind of contamination during inoculation in the laminar air flow chamber. In order to ensure the healthy growth of plants under in vitro conditions, cultures of *V. radiata* were maintained at 42% humidity, 26 °C–28 °C

temperature and 47 μmol m^{-2} s^{-1} photosynthetic photon flux density with 16 h light illumination and 8 h dark period. These conditions were maintained to mimic the natural environmental conditions.

The effect of a large range of concentrations of Bare TiO_2 and SDS-TiO_2 on seed germination and plant growth were studied by observing change in various morphological parameters like percentage seed germination, day of appearance of the radical root elongation, number of root laterals, shoot elongation, vigor index I, number of leaves, and their color change. Observations were recorded every day. The first observation was recorded a day after inoculation, and subsequent readings were taken each day for 6 days. Seeds were germinated in test tubes in water agar media containing 50 to 1000 mg L^{-1} NPs in each case separately. According to USEPA guidelines (USEPA 1996), seeds with roots longer than 5 mm were considered germinated. According to the International Seed Testing Association (ISTA), seed vigor is defined as the sum of those properties which determine the potential level of activity and performance of the seed or a seed lot during germination and seedling emergence. Seedling vigor was calculated using the following Eq. 4 (Feizi et al. 2012):

$$Vigor\ Index\ I = Germination\% \times seedling\ length\ (root + shoot)$$
$$(4)$$

Statistical analysis

Statistical significance was determined using a one-way analysis of variance (ANOVA) with SPSS 19.0 statistical software. The mean values for each treatment were compared using the Duncan's new multiple range test at $p \leq 0.05$. All analyses in case of cadmium removal were conducted with three replicates and two replicates in case of phytotoxicity studies. The results are presented as mean ± standard deviation (SD), and a confidence interval of 95% ($p < 0.05$) was considered significant in all cases.

Results and discussions

X-ray diffraction studies

Figure 2(a-c) depicts X-ray diffraction patterns of Bare-TiO_2, CTAB-TiO_2, and SDS-TiO_2 powders, respectively. The patterns have been normalized to enable a better comparison.

It could be clearly seen that all the diffraction peaks could be indexed to TiO_2 alone as there are no peaks of any other form of TiO_2 and/or any of the surfactants and their mixtures.

Fig. 2 XRD of (**a**) Bare TiO₂, (**b**) CTAB-TiO₂, and (**c**) SDS-TiO₂
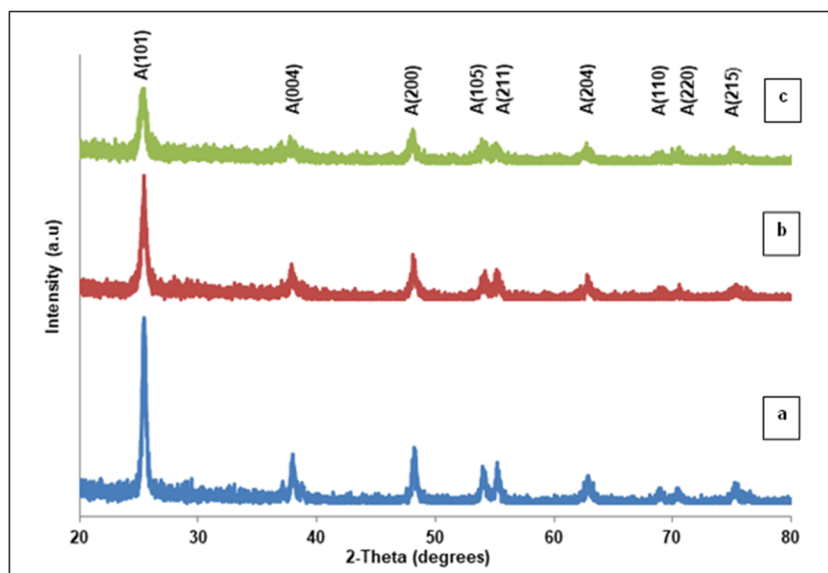
This further confirms that the system is devoid of surfactants, and it is pure TiO₂, obtained after synthesis in all cases. For all samples (101), (004), (200), (105), (211), (204), (110), (220) and (215) diffraction peaks appearing at 2θ values of 25.28⁰, 37.80⁰, 48.04⁰, 53.89°, 55.06°, 62.68°, 68.76°, 70.23°, and 75.13°, respectively, matches well with the standard TiO₂ diffraction pattern and identified as the anatase phase of TiO₂ (ICDD, International Centre for Diffraction data, File No. 21–1486) (Bahadur et al. 2010).

Such phase pure anatase TiO₂ as the result of surfactant modification has also been reported by Sharma et al. 2014 (Sharma and Lee 2014), Waseem et al. 2017 (Waseem et al. 2017) and Zha et al. 2014 (Zha et al. 2014). It is important to note that at 550 °C annealing temperature, there is no rutile phase present in any of the three materials. The probable reason could be the preference of having anatase over rutile owing to higher thermodynamic stability of the former, which is primarily a function of particle size, i.e., when particle size falls around 14 nm, the preferred phase is anatase (Bahadur et al. 2012).

Further, pure titania has been obtained irrespective of the kind of surfactant, i.e., cationic or anionic; however, it is important to know whether the type of surfactant has any role to play in the crystallite size and the intensity of diffraction peaks. To investigate this aspect, the Debye–Scherrer formula has been utilized, and the average crystallite size (D) of these particles have been estimated and found to be 4.284 nm in Bare TiO₂, which increased to 4.697 nm in CTAB-TiO₂ and decreased to 3.203 nm in SDS-TiO₂. These values of crystallite sizes in three cases is less than those reported by Rashad and Shalan 2013 for the hydrothermally synthesized bare and surfactant-assisted titania nanopowders (Rashad and Shalan 2013).

The values of lattice parameters a and c were calculated in all three cases individually by employing Eq. 5

$$\frac{1}{d^2} = \frac{4}{3}\left(\frac{h^2 + hk + k^2}{a^2}\right) + \frac{l^2}{c^2} \tag{5}$$

where d is the obtained lattice spacing for the diffraction peak (hkl) of the hexagonal lattice of TiO₂ (Bahadur et al. 2010). In all cases, diffraction peaks (1 0 1) and (2 0 0) of the hexagonal lattice of TiO₂ were used. The calculated values are tabulated in Table 1.

There was not much change in the values of lattice parameters "a" and "c" in cases of Bare TiO₂ and CTAB-TiO₂, as compared to SDS-TiO₂ where there is some increase in the value of lattice parameter. To the best of our knowledge, there is no such compilation of calculated values of lattice parameters of surfactant-modified titania nanomaterials.

Concerning the crystallite size of the produced nanoparticles, there is a strong dependence on the chemical structure and hydrocarbon chain length of the surfactants. Each surfactant has a characteristic critical micelle concentration (CMC) above which these forms micelles and the radius of these micelles are equal to the hydrocarbon chain length of the

Table 1 Lattice parameters and crystallite size of bare and surfactant modified TiO₂

Sample	d (Å)	a (Å)	c (Å)	D (nm)
Bare TiO₂	3.525	3.640	9.531	4.284
CTAB-TiO₂	3.525	3.640	9.530	4.697
SDS-TiO₂	3.533	3.649	9.590	3.203

surfactants (Bricha et al. 2012). Since the average size of CTAB micelle is expected to be greater than that of SDS micelles, therefore nanoparticles with larger crystallite size are obtained in case of CTAB-TiO$_2$, while the decrease in crystallite size is observed in case of SDS-TiO$_2$.

Regarding crystallinity, Bare TiO$_2$ having sharp and high-intensity peak indicates highest crystallinity among three materials. Surfactant modification has led to decrease in intensity and broadening of diffraction peaks together with poor peak separation, as distinctly shown in case of SDS. Such an observation of having an inhibitory effect on the overall crystallization process using ionic surfactants has also been reported by Bricha et al. 2012 (Bricha et al. 2012).

Fourier-transform infrared spectroscopy (FTIR)

The FTIR spectra in the range 4000–400 cm^{-1} is presented in Fig. 3(a–c), which provides further insight on the formation of titania in all cases. All three spectra appear identical, indicating similar nature, constitution, and composition of all three powdered materials with characteristic bands assigned to titania.

The presence of Ti–O–Ti bond could be confirmed from the bands between 581.69–745.81 cm^{-1}, assigned due to stretching vibration mode of TiO$_2$. These results are consistent with those reported by Zha et al. 2014 (2014). The bands at 3400 cm^{-1} originated due to O–H stretching vibration mode of water and at 1520 cm^{-1} due to the O-H bending of water indicate the presence of small amount of water adsorbed over TiO$_2$ surface. Such stretching vibrational modes of water are in line with those reported by Sharaf El-Deen and Zhang (2016).

The highly sensitive FTIR results indicated that no surfactant molecules eventually remained in the samples after the heat treatment at 550 °C, as the melting point of surfactants SDS and CTAB being 206 °C and around 240 °C, respectively (ICSC database: International Chemical Safety Cards). The nonexistence of CTAB and SDS after calcination is further confirmed when two prominent bands at 2850 and 2918 cm^{-1}, which are characteristic of strong bands for symmetric [$\nu_s(CH_2)$] and antisymmetric [$\nu_a(CH_2)$]CH$_2$ stretching modes of the alkyl chains of CTAB and 2851 and 2922 cm^{-1} for SDS, were found missing in the present FTIR spectra of prepared materials. Tah et al. 2011 also reported bands for CTAB and SDS at same positions (Tah et al. 2011).

Scanning electron microscopy

The surface morphology of the synthesized bare and surfactant-modified TiO$_2$ is exemplified in the scanning electron microscopy (SEM) micrographs of Bare TiO$_2$, CTAB, and SDS-modified TiO$_2$ in Fig. 4a–c, respectively.

From the micrographs (at same magnification), it is evident that Bare TiO$_2$ is irregular in shape whereas modification with surfactants has refined morphology to smooth, regular, and spherical-shaped particles. Similar kind of improvement in morphology as the result of surfactant modification was reported by Rashad and Shalan (2013) and Liu et al. 2007 (Liu et al. 2007).

Transmission electron microscopy

Transmission electron microscopy (TEM) is used to further examine nanoparticle size of the synthesized materials. Figures 5 (a–c), 6 (a–c), and 7(a–c) elucidate TEM micrographs, histograms depicting particle size distribution and selected area electron diffraction patterns (SAEDPs) for Bare TiO$_2$, CTAB-TiO$_2$, and SDS-TiO$_2$, respectively. Refinement

Fig. 3 FTIR spectra of (**a**) Bare TiO$_2$, (**b**) CTAB-TiO$_2$, and (**c**) SDS-TiO$_2$
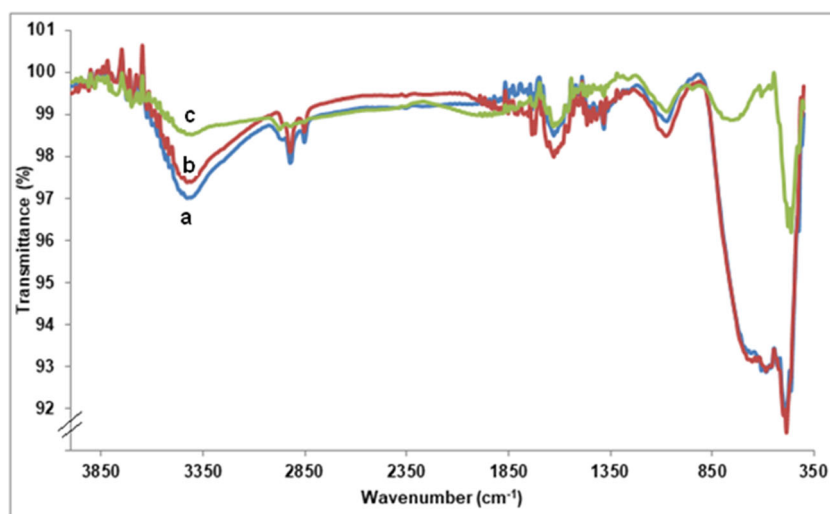
Fig. 4 SEM images of (**a**) Bare TiO$_2$, (**b**) CTAB-TiO$_2$, (**c**) SDS-TiO$_2$
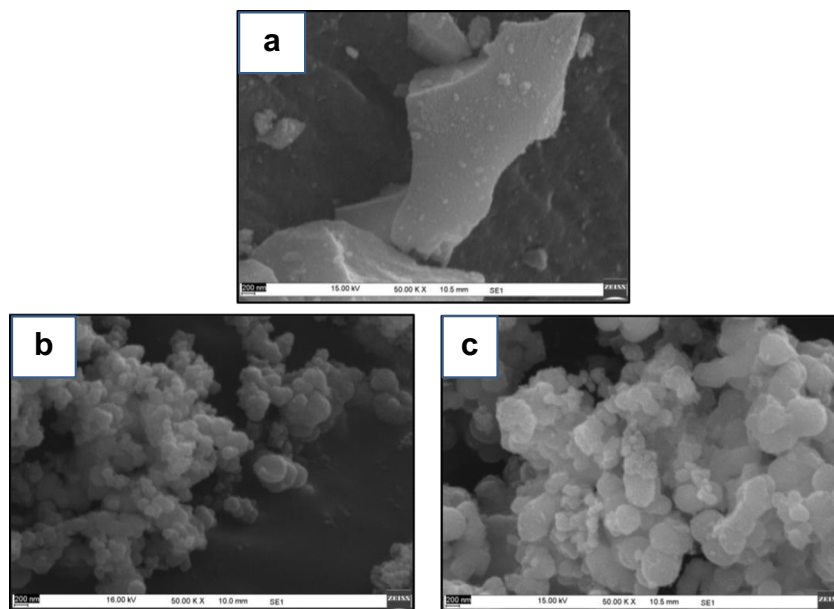
is evident with larger and irregular shape particles in Bare TiO$_2$ to more spherical shape and small size particles in case of both surfactant modifications. The average particle size in case of Bare TiO$_2$ was determined to be 14 nm, decreased to 11 nm in case of CTAB modification, and further decreased to 8 nm in case of SDS modification. The SAEDPs obtained in all cases corresponds to anatase phase of TiO$_2$.

Brunauer-Emmett-Teller (BET) surface area measurements

A set of nitrogen gas adsorption/desorption isotherm tests were carried out to evaluate the specific surface area (S$_{BET}$), pore size distribution, and total pore volume (V$_P$) for Bare TiO$_2$, CTAB, and SDS-modified materials using BET method and BJH desorption isotherms. The N$_2$ adsorption–desorption isotherms with the corresponding pore size distribution (in

inset) are depicted in Fig. 8 (a–c). All samples showed identical isotherms of type IV H2 hysteresis loop, characteristic of mesoporous materials. Further, the ratio of neck-to-body diameter increased from Bare TiO$_2$ to surfactant-modified TiO$_2$, indicating formation of more uniform, regular, and ordered pores. Thus, formation of TiO$_2$ organic core/surfactant organic shell structure leading to spherical morphology clearly demonstrates the role of surfactants as particle growth templates as titania solution is otherwise known to form agglomerated structures with bottleneck type pores (Choi et al. 2010; Alothman 2016). Also this analysis and discussion corroborate our findings from SEM and TEM analysis, where irregular shape morphology in Bare TiO$_2$ is refined with surfactant modification.

The specific surface area of bare TiO$_2$ was determined to be 22 m^2 g^{-1} with pore volume of 0.099 m^3 g^{-1} and bimodal pore size distribution in the range of 20–30 Å and 70–90 Å, with
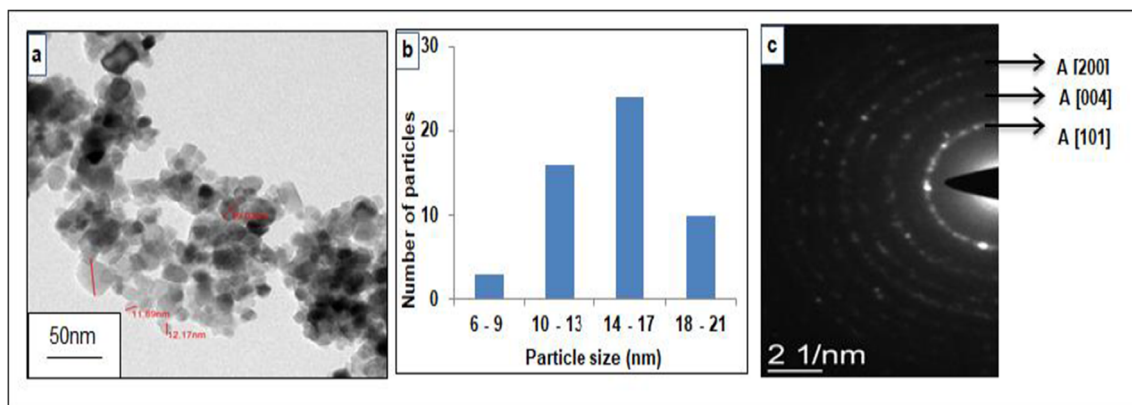
Fig. 5 TEM analysis of Bare TiO$_2$: (**a**) TEM micrograph, (**b**) particle size distribution, (**c**) SAEDP
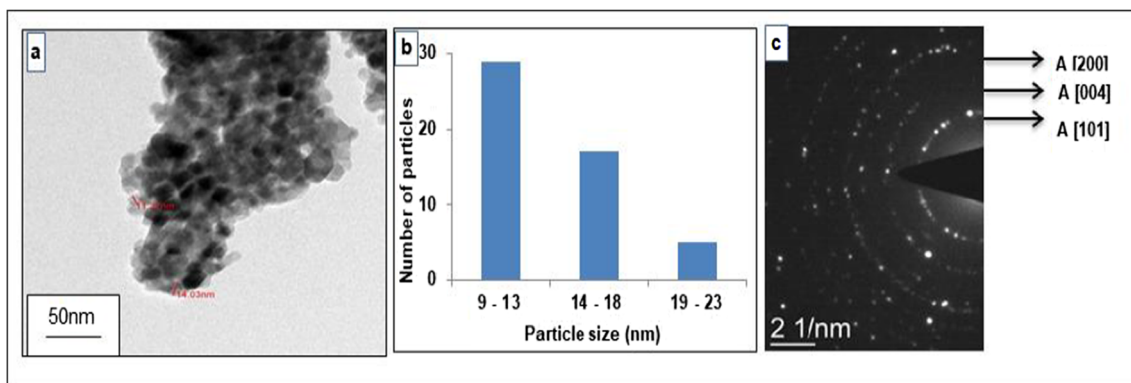
Fig. 6 TEM analysis of CTAB TiO$_2$: (**a**) TEM micrograph, (**b**) particle size distribution, (**c**) SAEDP

average pore size of 22 Å and 75 Å (inset Fig. 8). The TiO$_2$-CTAB sample showed almost four times increase in specific surface area to 85.54 m^2 g^{-1} with pore volume of 0.226 m^3 g^{-1} and bimodal pore size distribution in the similar range as bare, with average size around 18 Å and 70 Å. In case of TiO$_2$-SDS, specific surface area increased to almost three times to 66.77 m^2 g^{-1} and pore volume of 0.234 m^3 g^{-1}. In this case, the pore size distribution was wider in the range of 20–30 Å and 70–130 Å with average pore size of 25 Å and 95 Å. This increase in surface area due to surfactant modification in hydrothermally synthesized titania is also reported by Rashad and Shalan 2013 where the specific surface area was increased from 77.14 m^2 g^{-1} without surfactant to 78.59 m2/g in the presence of CTAB and 177.19 m^2 g^{-1} with SDS as anionic surfactant (Rashad and Shalan 2013).

Cadmium removal efficiency over different materials

The average Cd removal efficiency over different materials (Bare TiO$_2$, SDS-TiO$_2$, and CTAB-TiO$_2$) at varying concentrations of cadmium, i.e., 1, 3, 5, 9, and 12 mg dm^{-3} was studied in triplicate, and % Cd removal in each case

was calculated and has been tabulated in Table 2. From the data, significant differences ($p < 0.05$) in CTAB-TiO$_2$ and SDS-TiO$_2$ could be observed with respect to Bare TiO$_2$. The values in parenthesis are the relative standard deviation % in each case. The results indicate that all three materials proved beneficial towards cadmium removal. For all concentrations, both CTAB-TiO$_2$ and SDS-TiO$_2$ showed higher percentage removal as compared to Bare TiO$_2$, while modification with SDS led to highest percentage removal. The probable reason could be higher surface area and better porosity of surfactant-modified TiO$_2$ in particular SDS-TiO$_2$.

Adsorption of Cd on bare TiO$_2$ and SDS-TiO$_2$

To know the nature and extent of adsorption of Cd on bare and SDS-modified titania NMs, adsorption studies were undertaken. Figure 9 represents adsorption isotherms of cadmium on Bare TiO$_2$ and SDS-TiO$_2$. It may be seen that the two isotherms are essentially of similar nature and match to Type II isotherm. In both cases the amount of adsorbed Cd increases linearly in the beginning up to about 5 mg dm^{-3} of Cd, and at further higher concentrations, a secondary adsorption is
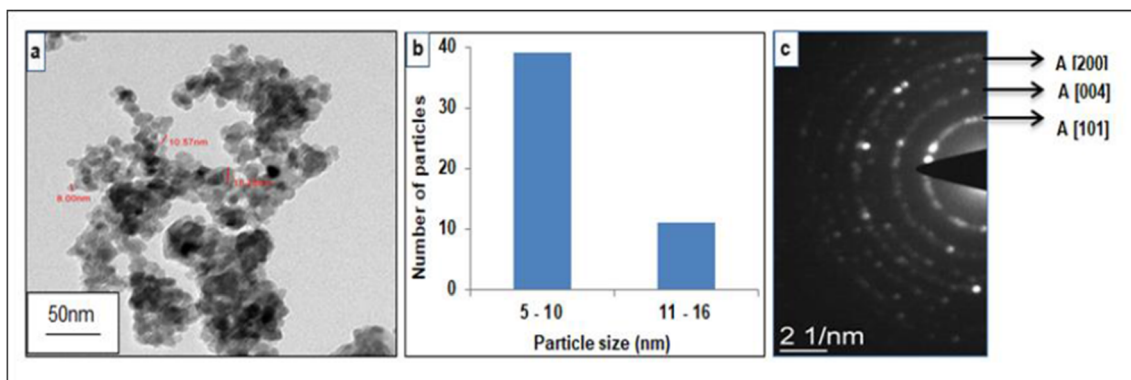
Fig. 7 TEM analysis of SDS-TiO$_2$: (**a**) TEM micrograph, (**b**) particle size distribution, (**c**) SAEDP

Fig. 8 N$_2$ adsorption–desorption isotherms with the corresponding pore size distribution curves of (**a**) Bare TiO$_2$, (**b**) CTAB-TiO$_2$, (**c**) SDS-TiO$_2$
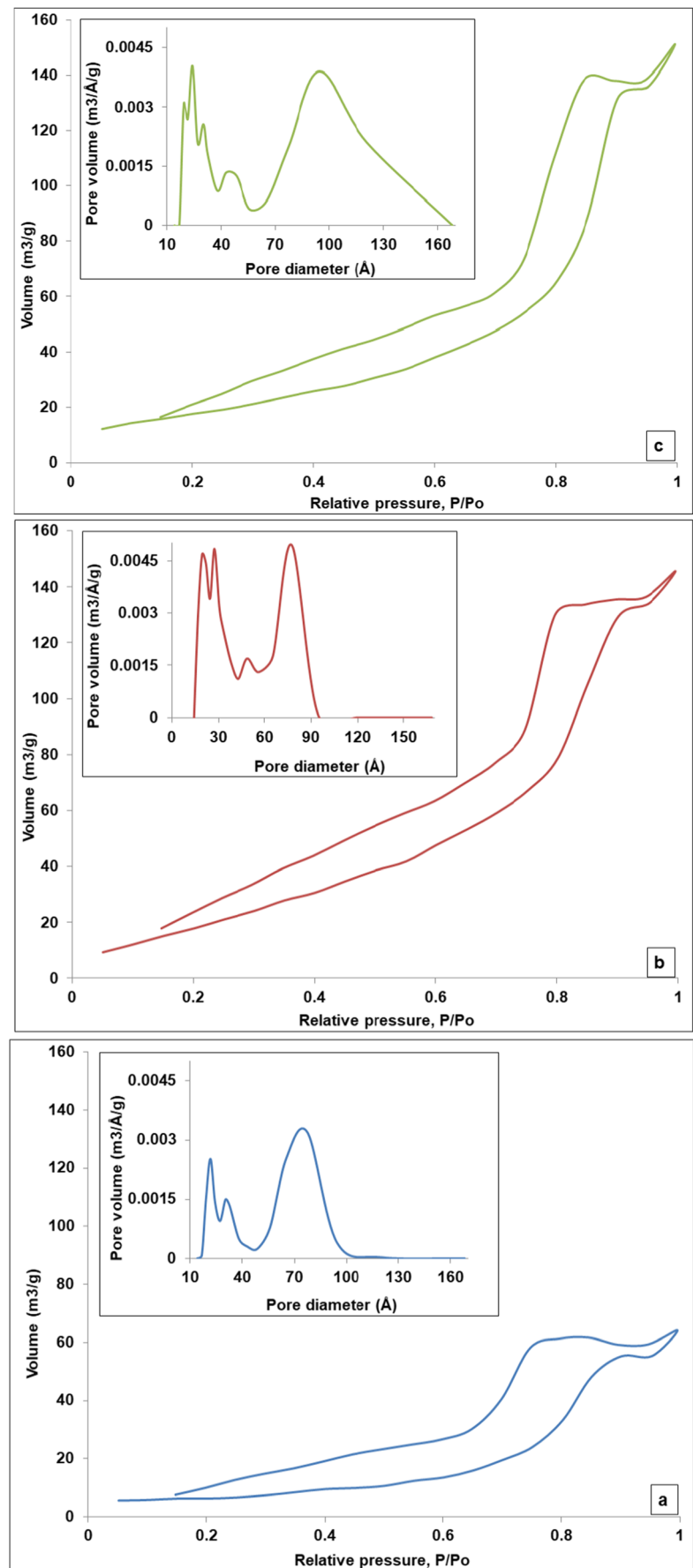
Table 2 Cd removal efficiency and relative standard deviation of (**a**) Bare TiO$_2$, (**b**) CTAB-TiO$_2$, and (**c**) SDS-TiO$_2$ (where, $p < 0.05$)

Cadmium concentration (mg dm^{-3})	Average removal of Cadmium (%) (relative standard deviation %)		
	Bare TiO$_2$	CTAB-TiO$_2$	SDS-TiO$_2$
1	75.05 (12.8)	91.86 (18.1)	95.42 (12.7)
3	76.65 (8.3)	92.93 (11.4)	98.93 (15.3)
5	82.88 (7.8)	94.69 (7.6)	99.56 (4.3)
9	88.92 (4.1)	93.59 (6.5)	96.63 (1.8)
12	90.00 (3.3)	93.78 (2.8)	98.98 (3.2)

ensured which increases exponentially from 7 to 12 mg dm^{-3}. At lower concentrations of Cd, in both cases, the adsorption isotherms appears to be of Type I, and the adsorption might be similar to that of Langmuir isotherm. The Langmuir plots (1/[Cd]$_{ad}$ vs 1/[Cd]$_{eq}$) for both systems have been shown in Fig. 9 (curves a and b), respectively.

The Langmuir plots for the two cases are linear, which indicate that in the lower concentration range (up to about 5 mg dm^{-3}), the adsorbed Cd forms monolayer on the surface of the catalyst and the adsorption follows Langmuir equation. From the intercepts of these linear plots, the capacity of adsorbent corresponding to monomolecular layer formation of cadmium was found to be 0.2027 and 0.3996 mg dm^{-3}, for Bare TiO$_2$ and SDS-TiO$_2$, respectively. The higher adsorption capacity with SDS-TiO$_2$ which is almost 2 times higher than

Bare TiO$_2$ may be attributed to improved morphology with higher surface area and higher pore volume obtained as the result of SDS modification.

This finding is supported by a report by Waseem et al. 2016 in which it can be seen that the maximum percent Cd^{2+} adsorption by SiO$_2$, TiO$_2$, and their nanocomposite at 300 °C was found to be 88, 92, and 96%, respectively. The adsorption of Cd^{2+} ions onto nanocomposite was higher than its counterparts which may be due to the presence of combined surface active groups like Si–H, Si–O–Ti and Ti–OH, and anatase phase of TiO$_2$ (Waseem et al. 2016).

Photocatalytic degradation of MB

Figure 10 shows UV-Vis spectrophotometric analysis depicting photocatalytic degradation in terms of decolorization efficiency of MB dye under 30 min solar light irradiation. The optimized conditions were pH 9.2, adsorbent dose 0.1 g, 30 min light exposure, and 1×10^{-5} M dye concentration at room temperature. When using photolysis alone (no nanomaterial), the degradation was 29%, whereas in presence of photocatalyst, the degradation percentage increased to 62% with Bare TiO$_2$, which further enhanced to 72% with CTAB-TiO$_2$ and 90% with SDS-TiO$_2$. These results are superior to those reported by Honarmand et al. 2019 where sodium bis(2-ethylhexyl)sulfosuccinate was used as surfactant for modification of TiO$_2$ to degrade MB dye with 76% efficiency in 300 min UV irradiation (Honarmand et al. 2019). Certainly 30 min solar light irradiation with 90% MB degradation efficiency as obtained in our case is attributed to improved morphology, enhanced surface area, higher adsorption leading to higher photocatalytic oxidation.

Fig. 9 Adsorption isotherms of cadmium at the interface of (**a**) bare TiO$_2$ and (**b**) SDS-TiO$_2$ (inset) Langmuir plot (1/[Cd]$_{ad}$ vs 1/[Cd]$_{eq}$) for each case
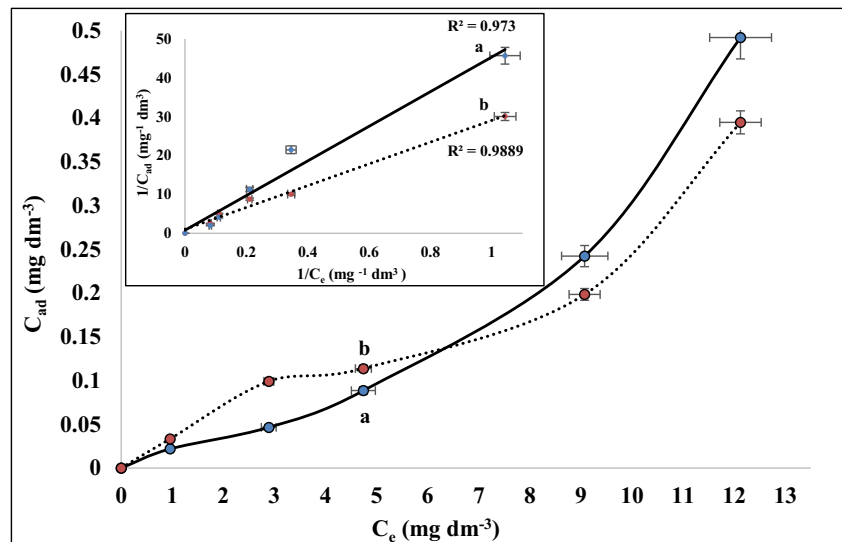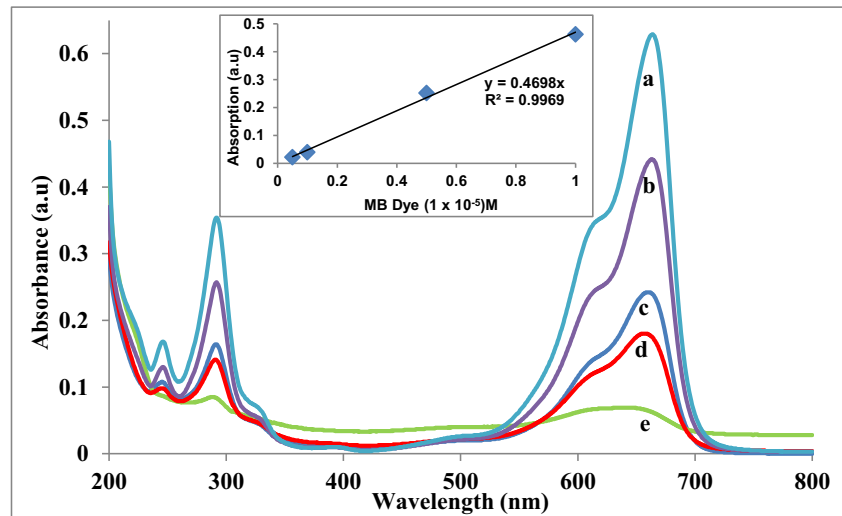
Fig. 10 MB dye degradation: (**a**) pure MB, (**b**) photolysis alone, (**c**) photocatalysis with Bare TiO₂, (**d**) with CTAB-TiO₂, and (**e**) with SDS-TiO₂ (inset) calibration curve of MB dye

Treatment of real textile and dyeing industry wastewater

Figure 11 shows the change in UV-vis spectra of the pre- and post-treated sample along with their respective photographs in the in-set. The results of pre- and post-treated wastewater quality parameters are tabulated in Table 3.

It is evident that the treatment leads to complete decolorization and deodorization of the sample. Also the treatment led to water quality, which met the Indian standards of discharge in surface water bodies, as laid down by pollution regulatory authority, Central Pollution Control Board (CPCB), Govt. of India. With the substantial reduction in TDS, TSS, and COD, the treated water could also be reused in the process.

Phytotoxicity test

In the present study, the effects of different concentrations (50 mg L^{-1}, 100 mg L^{-1}, 250 mg L^{-1}, 500 mg L^{-1} and 1000 mg L^{-1}) of Bare- and SDS-modified TiO₂ with respect to control on seed germination and overall growth of *Vigna radiata* (mung bean) were investigated and changes in various physiological properties like percentage seed germination, root length, shoot length, vigor index of seeds, color, and number of leaves were calculated and tabulated with pictures in Fig. 12. The seed germination test was conducted and relative seed germination rate, relative root growth, and germination index were calculated using Eqs. (1–3). The calculated data is tabulated in Table 4. All reported values were statistically significant according to Duncan's test ($p < 0.05$).

Fig. 11 UV-vis spectra of (**A**) pre- and (**B**) post-treated sample; respective photographs in the in-set
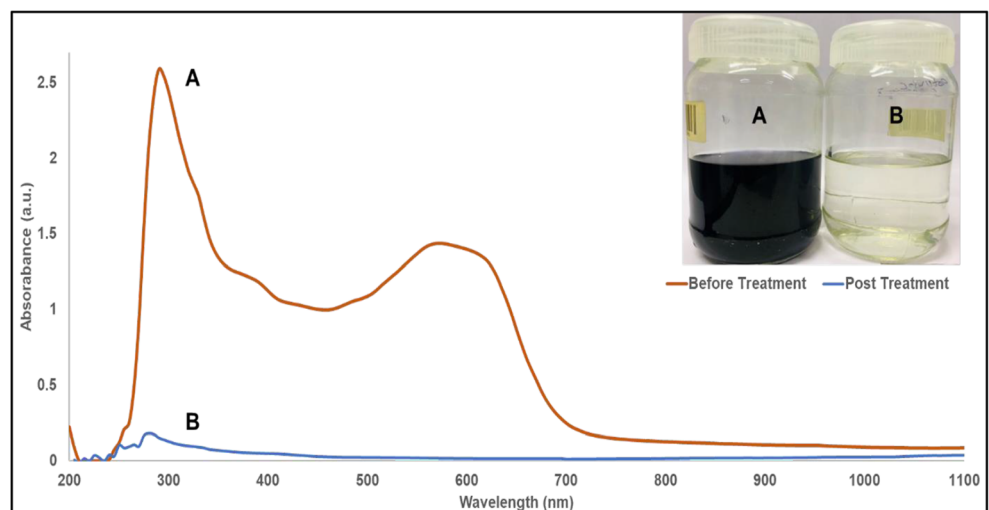
Table 3 Wastewater quality parameters for (A) pre- and (B) post-treated sample

Parameter	Untreated effluent (A)	Post-treated (B)	% Removal	CPCB standards for surface discharge
pH	10.3	9.5	–	6.5–8.5
Conductivity (μmho/cm)	5144	2925	43.14	–
Total dissolved solids (mg L^{-1})	2566	1459	43.14	2100
Total suspended solids (mg L^{-1})	1800	140	92.22	100
Total solids (mg L^{-1})	3712	1232	66.81	–
Chlorides (mg L^{-1})	719.8	349.89	51.39	–
Chemical oxygen demand (COD) (mg L^{-1})	304	128	57.89	250

From the images in Fig. 12 and the seed germination test data provided in Table 4, we could see that all seeds, control as well as those exposed to nanomaterials were germinated; hence, germination percentage is 100. Plant growth is evident with time (days) as observed in all cases of nanomaterials. As compared to control, Bare and modified TiO_2 was found to respond better in terms of germination rate and plant growth parameters. Among the two types of titania nanomaterials, SDS modified showed faster germination rate and plant growth probably because the SDS modification lead to improved morphology, surface properties, and reduced particle size. Such an observation of n-TiO_2 activated carbon composite effecting *Vigna radiata* seed germination and plant growth which might have resulted in better penetration into seed husks. This penetration may break the husks to allow water and nutrient uptake ultimately leading to rapid seed germination and plant growth is also reported by Singh et al. (2016). A trend of two green leaves was observed in all cases. This is also evident by vigor index I which was 1163 in case of Bare TiO_2 and 1448 in case of modified TiO_2 on the 6th day of study.

We believe that along with improved morphology and surface properties, crystallinity and phase of titania also has an important role to play, i.e., pure anatase phase of titania is responsible for these positive effects on germination percentage and vigor index. Our findings are supported by the report from Dehkourdi and Mosavi 2013 where significant increase in the percentage of germination, germination rate index, root and shoot length, fresh weight, vigor index, and chlorophyll content of seedlings is assigned due to phase pure Anatase titania (Dehkourdi and Mosavi 2013).

Such a study holds importance when there are limited reports on pure and mixed phases of titania affecting germination and plant growth. There have been both positive and negative reports on the effect of anatase alone (Dehkourdi and Mosavi 2013; Abdul 2015; Fellmann and Eichert 2017; Kořenková et al. 2017), rutile alone (Liu et al. 2017) and mixture of anatase and rutile (Ruffini et al. 2011; Mandeh et al. 2012; Castiglione et al. 2014).

Further, TiO_2 nanoparticles are reported to enhance germination rate in various species of plants like *Vigna radiata* and *Solanum lycopersicum* (Singh et al. 2016). However it is important to ascertain a concentration up to which these nanomaterials promote plant growth. To find out such an optimum concentration in this study, mung seeds were exposed at lower concentrations of 50 mg L^{-1}, where it could be seen that all physiological parameters are higher in surfactant-modified titania (9.250 cm of root length) as compared to bare (6 cm of root length) and control (6.625 cm of root length). Such an observation of improved growth parameters at lower concentrations is supported by a study from Feizi et al. 2012 where shoot and seedling growth at 2 and 10 mg L^{-1} concentration of nano-TiO_2 were much higher than those of control and bulk TiO_2 at the same concentration (Feizi et al. 2012).

Further, as concentration increased to 100 mg L^{-1}, 250 mg L^{-1}, and 500 mg L^{-1}, the same trend of improved germination rate, plant growth parameters, and higher vigor index was maintained. Vigor index raised to 1536 in modified TiO_2 at the optimum concentration of 500 mg L^{-1}. The use of engineered titania nanoparticles with improved morphology and surface properties could probably be a new approach to overcome problems with seed germination in some plant species, particularly medicinal plants which have lower germination rate dormancy period. Probably the modified titania accelerated the process of seed germination and significantly shortened the germination time as compared to the control. However; Feizi et al. 2012 showed that at high concentrations (500 mg L^{-1}), there was inhibitory or no effect on wheat (Feizi et al. 2012).

At further higher concentration of 1000 mg L^{-1} in both cases of nanomaterials, the germination percentage was not found to be affected; however, the other plant growth parameters either remain unchanged or decreased as compared to control, i.e., vigor index reduced to 863. This finding of ours is also supported by Andersen et al. 2016 (Andersen et al. 2016), where with the increase in concentration of 1000 mg L^{-1} of TiO_2, a decrease in plant growth was observed.

There seems to be a lot of variation with regard to findings and reports on the extent of concentration range of engineered TiO_2 NM up to which germination and plant growth is
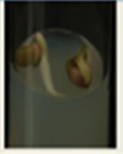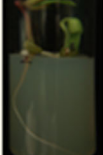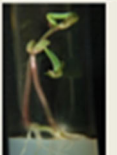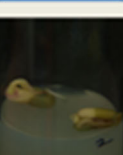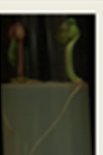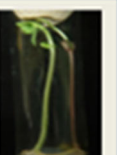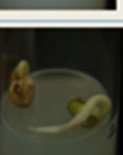
Fig. 12 Comparative table between control and different concentrations of Bare and SDS-TiO$_2$ after 5 h seed soaking pretreatment with a significant difference with respect to control ($p < 0.05$)

affected in a positive or a negative manner. It has been found that it varies with types (dicot/monocot), plant species, nature, constitution, and concentration of applied nanomaterials (Ruffini et al. 2011; Gerloff et al. 2012; Raliya et al. 2015; Andersen et al. 2016; Ji et al. 2016;

Singh et al. 2016; Rui et al. 2018). The detailed mechanism of transportation and fate of nanomaterials with the root and shoot system of plants has to be understood at the molecular level, for which further studies are undergoing and shall be reported shortly.

Table 4 Seed germination test

Sr. No.	Name of sample	Concentration of sample (mg L^{-1})	Relative seed germination Rate (%)	Relative root growth (%)	Germination index (%)
1	Bare TiO$_2$	50	100	90.56	110.42
		100	100	92.07	108.61
		250	100	93.58	106.86
		500	100	100	100
		1000	100	69.81	143.24
2	SDS-TiO$_2$	50	100	139.62	71.62
		100	100	128.30	77.94
		250	100	123.77	80.79
		500	100	132.07	75.71
		1000	100	64.15	155.88

Conclusion

Bare-, CTAB-, and SDS-modified TiO$_2$ was obtained using sol-gel synthesis. XRD and FTIR depicted identical spectra in all cases, which confirmed that both bare and surfactant-modified materials were pure TiO$_2$ with only anatase as the constituent phase and no surfactant remains with the materials. Surfactant modification led to improved morphology from irregular shape in Bare TiO$_2$ to regular spherical shape in both surfactant-modified TiO$_2$, as analyzed using SEM and TEM. Average particle size also reduced from 14 nm in Bare TiO$_2$ to 11 nm in case of CTAB-TiO$_2$, and 8 nm in SDS-TiO$_2$. BET surface area analysis provided type IV mesoporosity, with H2 hysteresis loop and increase in surface area to almost four times as the result of surfactant modification. The adsorption intensity of Cd on titania increased from 0.2027 mg dm^{-3} in Bare TiO$_2$ to 0.3996 mg dm^{-3} in SDS-TiO$_2$, which resulted in enhanced cadmium removal efficiency from 75.05% in Bare TiO$_2$ to 99.56% in SDS-TiO$_2$. Photodegradation of methylene blue dye under sunlight was carried out and decolorization efficiency enhanced from 62% with Bare TiO$_2$ to 72% with CTAB-TiO$_2$ and 90% with SDS-TiO$_2$. Under optimized conditions, the end-to-end treatment of real textile dyeing industry effluent led to meeting safe discharge norms as per CPCB, Govt. of India and also helped in achieving process water quality for efficient reuse. When evaluated towards possible toxicity and environmental safety, both Bare TiO$_2$ and SDS-TiO$_2$ showed safe seed germination (100% for all concentrations). With respect to control, root length changed from 6.625 cm to 8.750 cm, shoot length changed from 6.75 cm to 6.62 cm, and vigor index changed from 1338 to 1536 at 500 mg L^{-1} concentration of SDS-TiO$_2$ above this concentration the trend reversed and plant growth decreased. The use of engineered titania nanoparticles with improved morphology and surface properties could probably be a new approach to overcome problems with seed germination in some plant species, particularly medicinal plants which have lower germination rate dormancy period. Probably the modified titania accelerated the process of seed germination and significantly shortened the germination time as compared to the control. Along with improved morphology and surface properties, phase-pure anatase titania is established to be removing Cd, degrading MB dye, and treating textile wastewater together being environmentally safe for higher seed germination and plant growth.

Compliance with ethical standards

Conflict of interest The authors declare that they have no conflict of interest.

References

Abdul RDH (2015) Comparison the phytotoxicity of TiO$_2$ nanoparticles with bulk particles on Amber 33 variety of rice (*Oryza sativa*) in vitro comparison the phytotoxicity of TiO$_2$ nanoparticles with bulk particles on Amber 33 variety of rice (*Oryza sativa*) in vitro

Alothman ZA (2016) A review: fundamental aspects of silicate mesoporous materials. https://doi.org/10.3390/ma5122874

Andersen CP, King G, Plocher M, Storm M, Pokhrel LR, Johnson MG, Rygiewicz PT (2016) Germination and early plant development of ten plant species exposed to titanium dioxide and cerium oxide nanoparticles. Environ Toxicol Chem 35:2223–2229. https://doi.org/10.1002/etc.3374

Bahadur N, Bhargava N (2019) Novel pilot scale photocatalytic treatment of textile & dyeing industry wastewater to achieve process water quality and enabling zero liquid discharge. J Water Process Eng 32:100934. https://doi.org/10.1016/j.jwpe.2019.100934

Bahadur N, Jain K, Srivastava AK et al (2010) Effect of nominal doping of Ag and Ni on the crystalline structure and photo-catalytic properties of mesoporous titania. Mater Chem Phys 124:600–608. https://doi.org/10.1016/j.matchemphys.2010.07.020

Bahadur N, Pasricha R, Govind et al (2012) Effect of Ni doping on the microstructure and high curie temperature ferromagnetism in sol-gel derived titania powders. Mater Chem Phys 133:471–479. https://doi.org/10.1016/j.matchemphys.2012.01.068

Barrett-Lennard EG, Dracup M (1988) A porous agar medium for improving the growth of plants under sterile conditions. Plant Soil 108:294–298. https://doi.org/10.1007/BF02375663

Bricha M, Belmamouni Y, Essassi EM et al (2012) Surfactant-assisted hydrothermal synthesis of hydroxyapatite nanopowders. J Nanosci Nanotechnol 12:8042–8049. https://doi.org/10.1166/jnn.2012.6664

Cassiers K, Linssen T, Mathieu M et al (2004) Surfactant-directed synthesis of mesoporous titania with nanocrystalline anatase walls and remarkable thermal stability. J Phys Chem B 108:3713–3721. https://doi.org/10.1021/jp036830r

Castiglione MR, Giorgetti L, Cremonini R (2014) Impact of TiO2 nanoparticles on *Vicia narbonensis* L.: potential toxicity effects. https://doi.org/10.1007/s00709-014-0649-5

Chai L, Yu Y, Zhang G et al (2007) Effect of surfactants on preparation of nanometer TiO2 by pyrohydrolysis. Trans Nonferrous Met Soc China 17:176–180. https://doi.org/10.1016/S1003-6326(07)60068-5

Chawla S, Uppal H, Yadav M, Bahadur N, Singh N (2017) Zinc peroxide nanomaterial as an adsorbent for removal of Congo red dye from waste water. Ecotoxicol Environ Saf 135:68–74. https://doi.org/10.1016/j.ecoenv.2016.09.017

Choi H, Al-Abed SR, Dionysiou DD et al (2010) TiO2-based advanced oxidation nanotechnologies for water purification and reuse. In: Escobar I c., Schafer AI (eds) sustainable water for the future. Sustainability science and engineering 2:229–254

Dagher S, Soliman A, Ziout A, et al (2018) Photocatalytic removal of methylene blue using titania- and silica-coated magnetic nanoparticles Mater Res Express 5. https://doi.org/10.1088/2053-1591/aacad4

Dehkourdi EH, Mosavi M (2013) Effect of Anatase nanoparticles (TiO2) on parsley seed germination (*Petroselinum crispum*) in vitro. 283–286. https://doi.org/10.1007/s12011-013-9788-3

Delaide B, Goddek S, Gott J et al (2016) Lettuce (*Lactuca sativa* L. var. Sucrine) growth performance in complemented aquaponic solution outperforms hydroponics. Water (Switzerland) 8:1–11. https://doi.org/10.3390/w8100467

Dixit A, Mishra PK, Alam MS (2017) Titania nanofibers: a potential adsorbent for mercury and lead uptake. Int J Chem Eng Appl 8:75–81. https://doi.org/10.18178/ijcea.2017.8.1.633

Faraji J, Sepehri A (2018) Titanium dioxide nanoparticles and sodium nitroprusside alleviate the adverse effects of cadmium stress on germination and seedling growth of wheat (*Triticum aestivum* L.). Univ Sci 23:61–87. https://doi.org/10.11144/Javeriana.SC23-1.tdna

Feizi H, Rezvani Moghaddam P, Shahtahmassebi N, Fotovat A (2012) Impact of bulk and nanosized titanium dioxide (TiO2) on wheat seed germination and seedling growth. Biol Trace Elem Res 146:101–106. https://doi.org/10.1007/s12011-011-9222-7

Fellmann S, Eichert T (2017) Acute effects of engineered nanoparticles on the growth and gas exchange of *Zea mays* L. — what are the underlying causes? https://doi.org/10.1007/s11270-017-3364-y

Galkina OL, Vinogradov VV, Agafonov AV, Vinogradov AV (2011) Surfactant-assisted sol-gel synthesis of TiO2 with uniform particle size distribution. Int J Inorg Chem 2011:1–8. https://doi.org/10.1155/2011/108087

Ganguli D (1999) Sol-emulsion-gel synthesis of ceramic particles. Bull Mater Sci 22:221–226. https://doi.org/10.1007/BF02749923

Georgaka A, Spanos N (2010) Study of the Cu (II) removal from aqueous solutions by adsorption on titania. Glob NEST J 12:239–247

George R, Bahadur N, Singh N et al (2016) Environmentally benign TiO2 nanomaterials for removal of heavy metal ions with interfering ions present in tap water. Mater Today Proc 3:162–166. https://doi.org/10.1016/j.matpr.2016.01.051

Gerloff K, Fenoglio I, Carella E, Kolling J, Albrecht C, Boots AW, Förster I, Schins RP (2012) Distinctive toxicity of TiO2 rutile/Anatase mixed phase nanoparticles on Caco-2 cells. Chem Res Toxicol 25(3):646–655

Hattab A, Ahmed A, Hassan S, Ibrahim A (2017) Photocatalytic degradation of methylene blue by modified nanoparticles titania catalysts. 1210–1216. https://doi.org/10.1166/jnn.2017.12658

Honarmand MM, Mehr ME, Yarahmadi M, Siadati MH (2019) Effects of different surfactants on morphology of TiO2 and Zr-doped TiO2 nanoparticles and their applications in MB dye photocatalytic degradation. SN Appl Sci 1:505–512. https://doi.org/10.1007/s42452-019-0522-4

Imae T, Muto K, Ikeda S (1991) The pH dependence of dispersion of TiO2 particles in aqueous surfactant solutions. Colloid Polym Sci 269:43–48. https://doi.org/10.1007/BF00654658

Jaishankar M, Tseten T, Anbalagan N, et al (2014) Toxicity, mechanism and health effects of some heavy metals. 7:60–72. https://doi.org/10.2478/intox-2014-0009

N. Jayarambabu, Kumari BS, Rao KV, Prabhu YT (2014) Germination and growth characteristics of mungbean seeds (*Vigna radiata* L.) affected by synthesized zinc oxide nanoparticles. Int J Curr Eng Technol 4:3411–3416

Ji Y, Zhou Y, Ma C, Feng Y, Hao Y, Rui Y, Wu W, Gui X, le VN, Han Y, Wang Y, Xing B, Liu L, Cao W (2016) Jointed toxicity of TiO2 NPs and cd to rice seedlings: NPs alleviated Cd toxicity and Cd promoted NPs uptake. Plant Physiol Biochem 110:82–93. https://doi.org/10.1016/j.plaphy.2016.05.010

Jiang F, Shen Y, Ma C et al (2017) Effects of TiO2 nanoparticles on wheat (*Triticum aestivum* L.) seedlings cultivated under super-elevated and normal CO2 conditions. PLoS One 12:e0178088. https://doi.org/10.1371/journal.pone.0178088

Kiser MA, Westerhoff P, Benn T, Wang Y, Pérez-Rivera J, Hristovski K (2009) Titanium nanomaterial removal and release from wastewater treatment plants. Environ Sci Technol 43:6757–6763. https://doi.org/10.1021/es901102n

Kořenková L, Šebesta M, Urík M, et al (2017) Physiological response of culture media-grown barley (*Hordeum vulgare* L.) to titanium oxide nanoparticles. 4710. https://doi.org/10.1080/09064710.2016.1267255

Kumar V, Bahadur N, Sachdev D et al (2014) Restructural confirmation and photocatalytic applications of graphene oxide-gold composites synthesized by Langmuir-Blodgett method. Carbon N Y 80:290–304. https://doi.org/10.1016/j.carbon.2014.08.067

Kurepa J, Paunesku T, Vogt S, Arora H, Rabatic BM, Lu J, Wanzer MB, Woloschak GE, Smalle JA (2010) Uptake and distribution of ultra-small anatase TiO2 alizarin red s nanoconjugates in Arabidopsis thaliana. Nano Lett 10:2296–2302. https://doi.org/10.1021/nl903518f

Larue C, Khodja H, Herlin-Boime N et al (2011) Investigation of titanium dioxide nanoparticles toxicity and uptake by plants. J Phys Conf Ser 304. https://doi.org/10.1088/1742-6596/304/1/012057

Liu GQ, Jin ZG, Liu XX, Wang T, Liu ZF (2007) Anatase TiO2 porous thin films prepared by sol-gel method using CTAB surfactant. J Sol-Gel Sci Technol 41:49–55. https://doi.org/10.1007/s10971-006-0122-9

Liu H, Ma C, Chen G et al (2017) Titanium dioxide nanoparticles alleviate tetracycline toxicity to Arabidopsis thaliana (L.). https://doi.org/10.1021/acssuschemeng.6b02976

Mandeh M, Omidi M, Rahaie M (2012) In vitro influences of TiO$_2$ nanoparticles on barley (Hordeum vulgare L .) Tissue Culture. 376–380. https://doi.org/10.1007/s12011-012-9480-z

McKay G, Otterburn MS, Sweeney AG (1980) The removal of colour from effluent using various adsorbents-III. Silica: rate processes. Water Res 14:15–20. https://doi.org/10.1016/0043-1354(80)90037-8

Nayana CH, Pushpa T (2016) Nano zero-valent Iron for the removal of color and chemical oxygen demand of textile effluent. Indian J Adv Chem Sci S1:236–238

Oyebanji OB, Nweke O, Odebunmi O et al (2009) Simple, effective and economical explant-surface sterilization protocol for cowpea, rice and sorghum seeds. African J Biotechnol 8:5395–5399. https://doi.org/10.5897/AJB09.923

Raliya R, Biswas P, Tarafdar JC (2015) TiO$_2$ nanoparticle biosynthesis and its physiological effect on mung bean (Vigna radiata L.). Biotechnol Reports 5:22–26. https://doi.org/10.1016/j.btre.2014.10.009

Rashad MM, Shalan AE (2013) Surfactant-assisted hydrothermal synthesis of titania nanoparticles for solar cell applications. J Mater Sci Mater Electron 24:3189–3194. https://doi.org/10.1007/s10854-013-1226-y

Ruffini M, Lucia C, Geri C, Cremonini R (2011) The effects of nano-TiO$_2$ on seed germination , development and mitosis of root tip cells of Vicia narbonensis L . and Zea mays L. 2443–2449. doi: https://doi.org/10.1007/s11051-010-0135-8

Rui M, Ma C, White J et al (2018) Metal oxide nanoparticles alter peanut (Arachis hypogaea L.) physiological response and reduce nutritional quality: a life cycle study. Environ Sci: Nano 5:2088–2102. https://doi.org/10.1039/C8EN00436F

Sharaf El-Deen SEA, Zhang FS (2016) Immobilisation of TiO$_2$-nanoparticles on sewage sludge and their adsorption for cadmium removal from aqueous solutions. J Exp Nanosci 11:239–258. https://doi.org/10.1080/17458080.2015.1047419

Sharma S, Kaur A (2018) Various methods for removal of dyes from industrial effluents - a review. Indian J Sci Technol 11:1–21. https://doi.org/10.17485/ijst/2018/v11i12/120847

Sharma A, Lee BK (2014) Cd(II) removal and recovery enhancement by using acrylamide-titanium nanocomposite as an adsorbent. Appl Surf Sci 313:624–632. https://doi.org/10.1016/j.apsusc.2014.06.034

Singh P, Singh R, Borthakur A, Srivastava P, Srivastava N, Tiwary D, Mishra PK (2016) Effect of nanoscale TiO$_2$-activated carbon composite on Solanum lycopersicum (L.) and Vigna radiata (L.) seeds germination. Energy. Ecol Environ 1:131–140. https://doi.org/10.1007/s40974-016-0009-8

Skubal LR, Meshkov NK, Rajh T, Thurnauer M (2002) Cadmium removal from water using thiolactic acid-modified titanium dioxide nanoparticles. J Photochem Photobiol A Chem 148:393–397. https://doi.org/10.1016/S1010-6030(02)00069-2

Tah B, Pal P, Mahato M, Talapatra GB (2011) Aggregation behavior of SDS/CTAB catanionic surfactant mixture in aqueous solution and at the air/water interface. J Phys Chem B 115:8493–8499. https://doi.org/10.1021/jp202578s

United States Environmental Protection Agency (USEPA), (1996) Ecological Effects Test Guidelines (OPPTS 850.4200): Seed Germination/Root Elongation Toxicity Test. https://doi.org/10.1016/j.buildenv.2013.04.024

Waseem M, Muntha ST, Nawaz M, et al (2016) Effect of heat treatment on the efficient adsorption of Cd^{2+} ions by nanosized SiO_2, TiO_2 and their composite. 0–23

Wei J, Wen X, Zhu F (2018, 2018) Influence of surfactant on the morphology and photocatalytic activity of anatase TiO$_2$ by solvothermal synthesis. J Nanomater. https://doi.org/10.1155/2018/3086269

Wu W, Zhang L, Zhai X et al (2018) Preparation and photocatalytic activity analysis of nanometer TiO$_2$ modified by surfactant. Nanomater Nanotechnol 8:1–8. https://doi.org/10.1177/1847980418781973

Zha R, Nadimicherla R, Guo X (2014) Cadmium removal in waste water by nanostructured TiO$_2$ particles. J Mater Chem A 2:13932–13941. https://doi.org/10.1039/C4TA02106A